NEURODEVELOPMENT

Prenatal activity from thalamic neurons governs the emergence of functional cortical maps in mice

Noelia Antón-Bolaños*, Alejandro Sempere-Ferràndez*, Teresa Guillamón-Vivancos, Francisco J. Martini, Leticia Pérez-Saiz, Henrik Gezelius†, Anton Filipchuk‡, Miguel Valdeolmillos, Guillermina López-Bendito§

The mammalian brain's somatosensory cortex is a topographic map of the body's sensory experience. In mice, cortical barrels reflect whisker input. We asked whether these cortical structures require sensory input to develop or are driven by intrinsic activity. Thalamocortical columns, connecting the thalamus to the cortex, emerge before sensory input and concur with calcium waves in the embryonic thalamus. We show that the columnar organization of the thalamocortical somatotopic map exists in the mouse embryo before sensory input, thus linking spontaneous embryonic thalamic activity to somatosensory map formation. Without thalamic calcium waves, cortical circuits become hyperexcitable, columnar and barrel organization does not emerge, and the somatosensory map lacks anatomical and functional structure. Thus, a self-organized protomap in the embryonic thalamus drives the functional assembly of murine thalamocortical sensory circuits.

The mammalian cerebral cortex is arranged into radial columns that coalesce during development. These columns become functionally organized before adulthood (*1*–*3*). Some evidence suggests that genetic factors regulate initial columnar patterning (*4*); other evidence suggests that functional maps arise postnatally as a result of sensory experience (*5*–*9*). However, spatially organized patterns of spontaneous activity are evident in the embryonic thalamus, before cortical neurons have completed their radial migration (*10*). One well-studied functional map is the somatotopic correspondence between whiskers and their associated clusters of layer 4 neurons (called barrels) in the rodent primary somatosensory cortex (S1) (*11*). Although barrels are apparent anatomically at postnatal day 4 (P4) (*12*), domains of spontaneously co-activated neurons can be identified at birth in S1 in vivo (*13*–*15*). We asked whether the emergence of anatomically discernable structures is preceded by organized activity in the mouse embryo. We discovered that structured patterns of neuronal activity in the embryonic thalamus define functional cortical columns and the concomitant functional somatotopic map in the immature cortex.

The functional properties of embryonic thalamocortical connections were assessed by recording the somatosensory cortical calcium responses elicited by the activation of the ventral posteromedial nucleus (VPM) of the thalamus in slices. By embryonic day 17.5 (E17.5), electrical stimulation of the VPM triggered calcium waves that propagated over a large area of the nucleus, resembling previously reported spontaneous activity (*10*). This thalamic stimulation elicited a cortical calcium response in the S1 (Fig. 1, A and B; fig. S1A; and movie S1). Whereas the activation of thalamocortical axons is confined to the subplate at this stage (fig. S1B), the cortical response spanned the entire thickness of the cortical plate, suggesting that thalamocortical axons activate a radially organized cortical network. From E18.5 onward, VPM stimulation activated a progressively restricted territory within the nucleus (fig. S1C), allowing us to define the functional topography of the nascent thalamocortical projection. Perithreshold stimulation of adjacent regions in the VPM activated distinct columnar territories in the cortex (Fig. 1, C and D), indicating the existence of a functional protomap present in these embryonic thalamocortical circuits. This was evaluated in vivo by transcranial calcium imaging of glutamatergic cortical neurons at E18.5. Mechanical stimulation of juxtaposed areas of the whisker pad activated discrete, segregated, and spatially consistent cortical territories in the contralateral S1 (Fig. 1, E and F, and movie S2), confirming the existence of a cortical somatosensory protomap in the intact embryo.

We then tested whether embryonic thalamic calcium waves influence the emergence of the functional cortical columns that presage the formation of the somatotopic barrel map. To change the normal pattern of spontaneous thalamic activity, we crossed a tamoxifen-dependent *Gbx2Cre^{ERT2}* mouse with a floxed line expressing the inward rectifier potassium channel 2.1 (Kir) fused to the mCherry reporter (fig. S2) (*10*). In this model (referred to hereafter as *Th^{Kir}*), 78% of the VPM neurons express Kir-mCherry protein upon tamoxifen administration at E10.5 (fig. S2). In control slices, more than half of the spontaneous synchronous events in the VPM corresponded to large-amplitude, highly synchronized calcium waves, whereas the remaining activity reflected low-amplitude, poorly synchronized events. The highly synchronized waves were not detected in the *Th^{Kir}* mice, in which only small-amplitude and mostly asynchronous activity persisted, although at a higher frequency than in controls (Fig. 2, A to C, and movies S3 and S4). Collectively, Kir overexpression shifted the pattern of spontaneous activity in the thalamus from synchronized waves to asynchronous activity.

At the cellular level, whereas control neurons were relatively depolarized at E16.5, *Th^{Kir}* cells displayed a bistable pattern of activity with spontaneously alternating periods of hyperpolarized and depolarized membrane potential (Fig. 2D and fig. S3). Action potentials were generated in the depolarized phase in both control and *Th^{Kir}* cells. This change in the electrical properties of the *Th^{Kir}* neurons was sufficient to impede the generation of calcium waves. Barium, an ion that blocks Kir channels (*16*), reversed the electrophysiological profile of *Th^{Kir}* neurons, recovering the wavelike activity in *Th^{Kir}* VPM networks (fig. S4 and movie S5). Thus, although there were no propagating calcium waves in the thalami of *Th^{Kir}* mice, the preservation of thalamic asynchronous activity meant that the thalamus was not silent.

We analyzed how altering the pattern of spontaneous thalamic activity in our *Th^{Kir}* model affected the functional columnar organization in S1. Perithreshold VPM stimulation in E17.5 to E18.5 slices from control mice triggered a columnar-like cortical response (fig. S5A and movie S6). Conversely, this stimulation in *Th^{Kir}* slices consistently elicited a broader (laterally) cortical calcium wave (fig. S5A and movies S7 and S8). Despite these differences, the subplate was the earliest cortical compartment activated in both control and *Th^{Kir}* mice, followed by the upper cortex (fig. S5, B to D). Next, we tested whether the emergence of the functional topographic map was affected in the *Th^{Kir}* mice. Stimulation of adjacent regions in the VPM in the *Th^{Kir}* slices, unlike that in the controls, activated highly overlapping territories in the cortex (Fig. 3A), indicating that the topographical representation of the thalamocortical circuit does not emerge in the absence of embryonic thalamic waves. Postnatally, the cortical response to VPM stimulation narrowed progressively with time in control slices, coinciding at P4 with the dimensions of the cortical barrel, yet this spatial restriction occurred to a lesser extent in the *Th^{Kir}* mice (Fig. 3, B and C, and movies S9 and S10). These differences were observed irrespective of the stimulation strength (fig. S6).

The extended cortical activation in the *Th^{Kir}* mice was not due to more extensive activation of the VPM (fig. S7), yet it was associated with increased levels of intrinsic cortical excitability. This was reflected by the high frequency of spontaneous cortical waves in *Th^{Kir}* slices (fig. S8,

Instituto de Neurociencias de Alicante, Universidad Miguel Hernández-Consejo Superior de Investigaciones Científicas (UMH-CSIC), Sant Joan d'Alacant, Spain.
*These authors contributed equally to this work. †Present address: Science for Life Laboratory, Tomtebodavägen 23A, 17165 Solna, Sweden. ‡Present address: Department of Integrative and Computational Neuroscience (ICN), Paris-Saclay Institute of Neuroscience (NeuroPSI), CNRS/University Paris-Sud, 91198 Gif-sur-Yvette, France.
§Corresponding author. Email: g.lbendito@umh.es

A and B) and the widespread cortical response to intracortical stimulation (fig. S8, C to E). Next, we tested whether this change in cortical network excitability occurred in the Th^{Kir} mice in vivo. Because cortical traveling waves were associated with action potential bursts (fig. S8F), we recorded extracellular cortical activity with multichannel electrodes. We found extensive spontaneous events of synchronous activity spreading horizontally in the Th^{Kir} mice at P2 to P3 (Fig. 3, D to F), consistent with the hyperexcitability observed ex vivo. We then analyzed the possible origin for this excitability and found that the amplitude of the calcium response was the same in the subplate but larger in the upper cortex in the Th^{Kir} mice (fig. S9), suggesting a local alteration in the upper cortical network. As metabotropic glutamate receptors (mGluRs) participate in the propagation of cortical spontaneous activity in newborn rodents (*17*, *18*), we tested whether mGluRs could be involved in the hyperexcitability of cortical networks in Th^{Kir} mice. Bath application of 2-methyl-6-(phenylethynyl)pyridine (MPEP) (100 μM), an mGlu5-specific antagonist, rescued the activation of the thalamocortically induced cortical network into a column-like domain in Th^{Kir} mice. Although MPEP decreased the overall signal intensity in both conditions, it had no effect on the width of the cortical response in controls (fig. S10, A to C). These results are consistent with increased expression of cortical mGlu5 in the Th^{Kir} mice at P0 (fig. S10D). Together, these data reveal that the emergence of functional columns and a somatotopic map in the S1 relies on thalamic control of cortical excitability, implicating mGluRs.

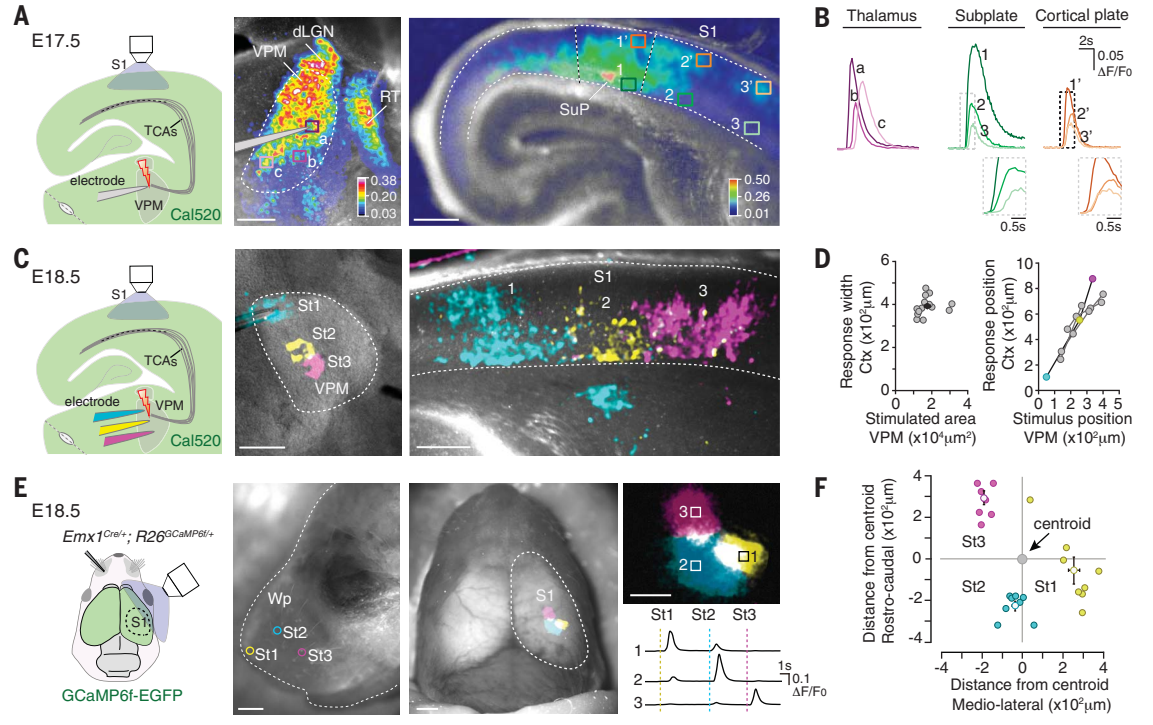

Fig. 1. Embryonic thalamocortical stimulation reveals an organized prenatal cortical map. (**A**) Experimental design. The maximal projection of the calcium responses [measured as the ratio of the change in fluorescence to the baseline fluorescence ($\Delta F/F_0$)] (color coded) in the VPM and cortex after VPM stimulation at E17.5 is shown. (**B**) Calcium transients from boxes in (A). (**C**) Experimental design. The maximal projection of cortical responses after the stimulation of three adjacent VPM regions (St1 to St3) at E18.5 is shown. (**D**) (Left) Plot of the stimulated VPM area versus the cortical response width (the black dot represents the mean value). (Right) Plot of the stimulus position in the VPM versus the cortical response location (n = 16 stimulation sites from 4 slices). Colored circles represent the data in (C). (**E**) Experimental design. Cortical calcium responses were elicited by mechanical stimulation of three contralateral whisker pad (Wp) sites (St1 to St3) at E18.5. (Right) High-magnification images and transients recorded in each region of interest (ROI) (boxes labeled 1 to 3). (**F**) Plot of the position of each cortical response relative to the centroid of the activated area (n = 8 mice). dLGN, dorsolateral geniculate nucleus; RT, reticular thalamus; SuP, subplate; TCAs, thalamocortical axons; Cal520, calcium indicator 520; Ctx, cortex; GCaMP6f-EGFP, calmodulin-based genetically encoded fluorescent calcium indicator 6–fast. Scale bars, 200 μm in (A), 1 mm in (E) (left and middle), and 500 μm in (E) (right).

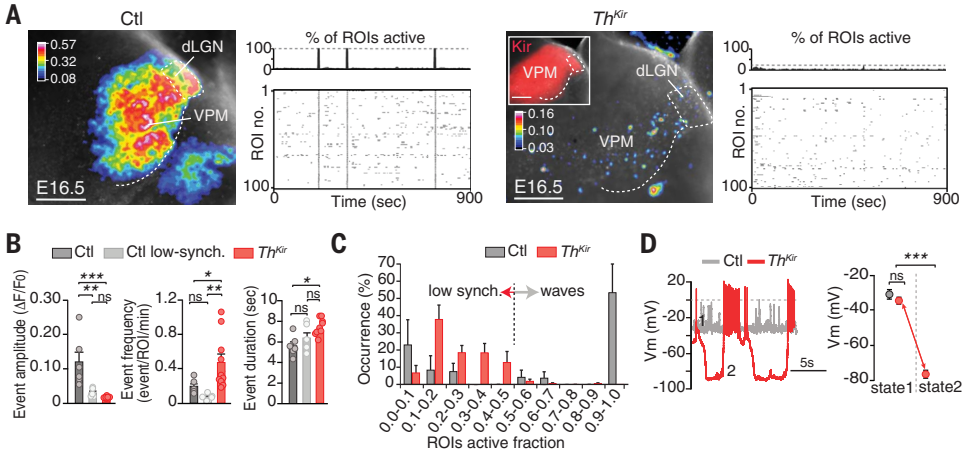

Fig. 2. Desynchronizing the embryonic thalamic pattern of activity. (**A**) Maximal projection of ex vivo spontaneous calcium activity in the VPM and accompanying raster plots for control (Ctl) and Th^{Kir} slices at E16.5. (**B**) Properties of the VPM calcium events (n = 6 control slices, n = 10 Th^{Kir} slices; ns, not significant; *P < 0.05, **P < 0.01, ***P < 0.001). (**C**) Percent distribution of active ROIs. (**D**) Representative traces and quantification of membrane potential (Vm) in control and Th^{Kir} neurons recorded at E16.5 to E18.5 (control, n = 7 slices; Th^{Kir}, n = 7 slices). ***P < 0.001. Scale bars, 200 μm. Data are means ± SEM.

To ascertain whether embryonic thalamic activity and functional columns are prerequisites to establish the postnatal anatomy of the barrel map, we examined thalamocortical axons clustering in the Th^{Kir} mice in which this projection was labeled by green fluorescent protein (GFP) (TCA-GFP mice) (*19*). The barrel map was evident at P4 in control mice (*12*, *20*), but no barrels were detected in tangential or coronal sections of Th^{Kir} mice, where thalamocortical axons targeted layer 4 but did not segregate into discrete clusters (Fig. 4A and fig. S11). Furthermore, there was no arrangement of layer 4 cells into barrel walls in the Th^{Kir} mice. The absence of barrels did not seem to originate from the loss of neurotransmitter

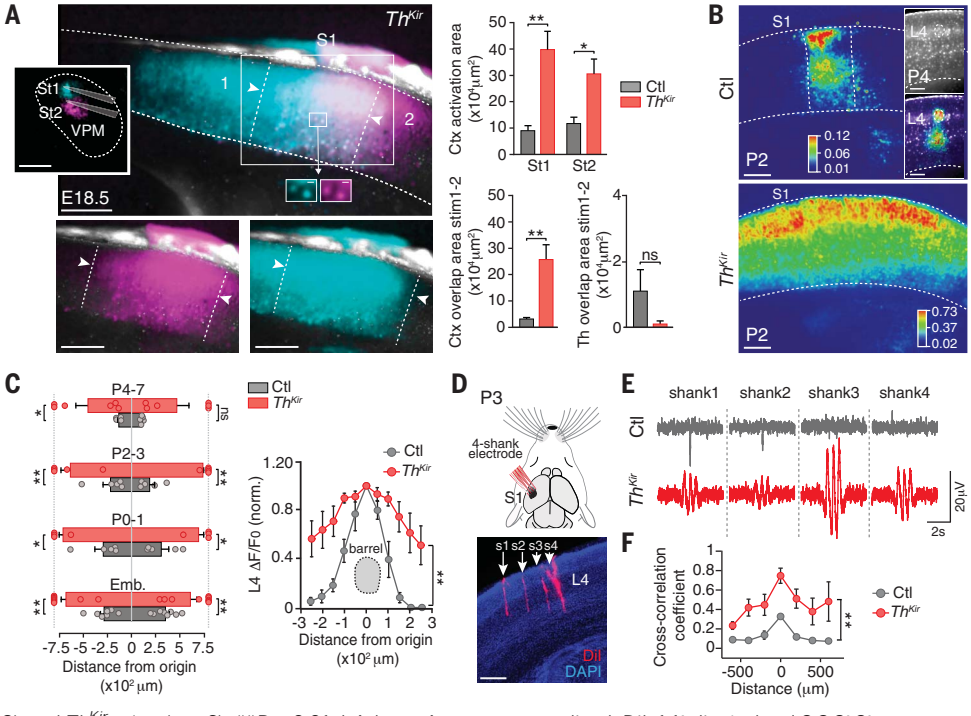

Fig. 3. Loss of functional cortical prebarrel columns in the Th^{Kir} mice. (**A**) Maximal projection of cortical responses after the stimulation (stim) of two adjacent VPM regions in Th^{Kir} slices. (Right) Quantifications of the activated area (n = 6 control slices, n = 6 Th^{Kir} slices; ns, not significant; *P < 0.05, **P < 0.01). Arrowheads indicate the cortical territory with overlapping activation. (**B**) Cortical activation elicited by VPM stimulation at P2 (inset, P4) in control (Ctl) and Th^{Kir} slices. (**C**) Quantification of the horizontal spread of the cortical response [E17 to E18 (emb.), n = 8 control slices, n = 9 Th^{Kir} slices; P0 to P1, n = 5 control, n = 4 Th^{Kir}; P2 to P3, n = 5 control, n = 5 Th^{Kir}; P4 to P7, n = 5 control, n = 6 Th^{Kir}; ns, not significant; *P < 0.05, **P < 0.01]. (Right) Same in layer 4 at P4 to P7 (n = 6 control slices, n = 6 Th^{Kir} slices; **P < 0.01). (**D**) Experimental design and coronal image showing the four-shank (s1 to s4) electrode insertion in S1 (red). (**E**) Representative in vivo recordings of spontaneous cortical network activity. (**F**) Quantification of the cross-correlation coefficient among shanks in control mice (n = 3) and Th^{Kir} mice (n = 6). **P < 0.01. L4, layer 4; norm., normalized; DiI, 1,1′-dioctadecyl 3,3,3′,3′-tetramethylindocarbocyanine perchlorate; DAPI, 4′,6-diamidino-2-phenylindole. Scale bars, 200 µm. Data are means ± SEM.

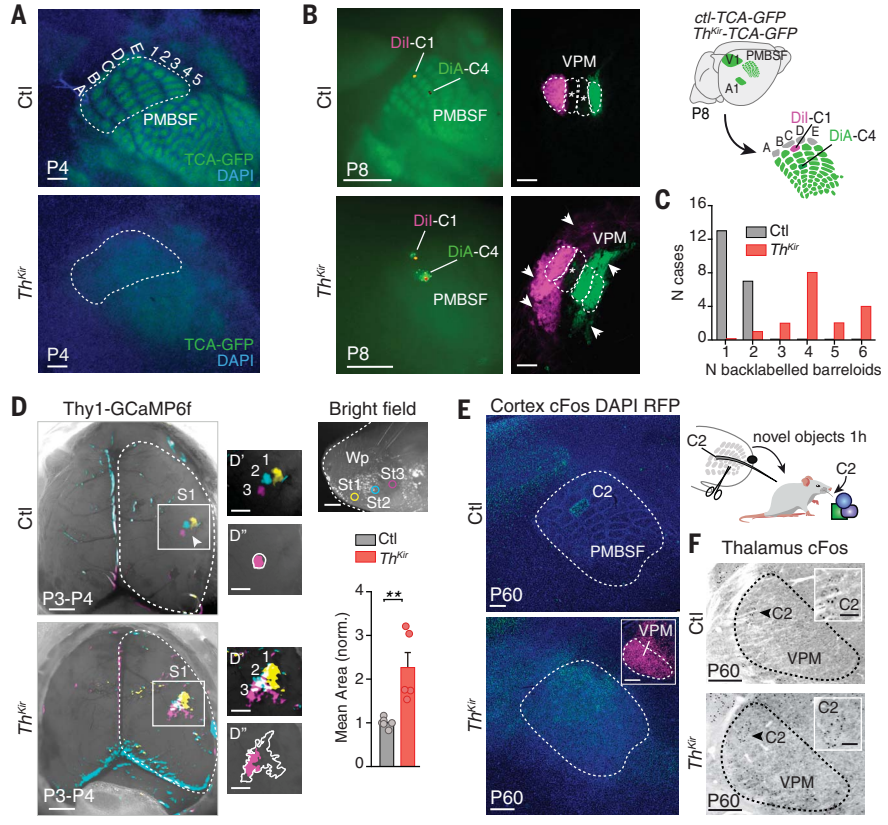

Fig. 4. Long-term anatomical and functional changes in S1 of the Th^{Kir} mice. (**A**) Tangential sections showing the posteromedial barrel subfield (PMBSF) in control (Ctl) and Th^{Kir} TCA-GFP mice at P4. Letters and numbers correspond to the diagram in (B). (**B**) Experimental design and images showing PMBSF injection sites and back-labeled barreloids in the VPM. Arrowheads show back-labeling outside the expected barreloids and asterisks indicate the non-back-labeled barreloids. (**C**) Quantification of data shown in (B) (n = 10 control slices, n = 10 Th^{Kir} slices). (**D**) Maximal projection of the in vivo contralateral cortical responses elicited by mechanical stimulation of three whisker pad (Wp) sites (St1 to St3) at P3 to P4 (top right). (D′) High-power views. (D″) Drawing of initial (pink) and maximal (outline) extension of representative responses. (Bottom right) Quantification of the data (n = 6 control mice, n = 5 Th^{Kir} mice; **P < 0.01). (**E**) Experimental design and cortical cFos immunostaining. (**F**) VPM cFos immunostaining. Scale bars, 300 µm in (A), (B) (right), (E), and (F) (insets, 100 µm); 1 mm in (B) (left) and (D) (insets, 500 µm). DiA, 4-Di-16-ASP (4-(4-(dihexadecylamino)styryl)-*N*-methylpyridinium iodide); A1, primary auditory cortex; V1, primary visual cortex; RFP, red fluorescent protein. Data are means ± SEM.

release (*21*, *22*), as thalamic neurons in the Th^{Kir} mice fire action potentials and activate synaptic currents in cortical cells (figs. S4A, S9D, and S12, A to C) and respond normally to whisker stimulation in vivo (fig. S12, D and E).

The disrupted barrel map in Th^{Kir} mice may reflect altered point-to-point connectivity at several subcortical levels (*8*, *23*, *24*). However, the organization of brainstem barrelettes and thalamic barreloids in the Th^{Kir} mice was normal (fig. S13). As the barrel map ultimately relies on the specific topographic organization of thalamocortical axons (*25*), we explored whether some spatial segregation was conserved in the Th^{Kir} mice. Although dye deposition in barrels C1 and C4 back-labeled cells in the corresponding barreloids of control mice, the back-labeled territories in Th^{Kir} mice were more extensive, including cells located in neighboring barreloids (Fig. 4, B and C). Anterograde tracing from single barreloids also revealed a broader horizontal disposition of thalamocortical axons in layer 4 of the Th^{Kir} mice (fig. S14). Lastly, we determined how this aberrant topographic map generated by the lack of thalamic calcium waves affected the relay of sensory stimuli in early postnatal mice in vivo. Whereas the stimulation of distinct points on the whisker pad at P3 to P4 activated discrete barrel-like patches in the control S1, similar stimulations of Th^{Kir} mice led to enlarged responses in the barrel field (Fig. 4D and movies S11 and S12). Together, these data demonstrate that the postnatal anatomic clustering of thalamocortical axons and the somatotopic functional map are disrupted in the absence of embryonic thalamic waves.

As the critical period of thalamocortical plasticity in the S1 closes between P3 and P7 in rodents (*6*, *20*, *26*), we assessed whether the loss of columnar organization in the Th^{Kir} mice could be overcome by sensory experience. The loss of barrel organization and the lack of a precise functional map persisted in adult Th^{Kir} mice, as indicated by vGlut2 (vesicular glutamate transporter 2) staining and the unrestrained cortical activation of cFos (Fig. 4E and fig. S15). The thalami of Th^{Kir} mice retained a normal functional topography when whiskers were stimulated (Fig. 4F). Hence, the natural period of somatosensory-driven plasticity cannot overcome the altered organization that occurs in the embryo.

Our data reveal that embryonic patterns of thalamic activity organize the architecture of the somatosensory map. We have shown that the development of this map involves the emergence of functional cortical columns in embryos, driven by spontaneous thalamic wavelike activity. These embryonic columns display spatial segregation and somatotopic organization, despite the immature state of the cortical sheet in which they materialize. We propose that patterned activity in precortical relay stations during embryonic stages prepares cortical areas and circuits for upcoming sensory input. As thalamic waves are not exclusive to the somatosensory nucleus but propagate to other sensory nuclei [e.g., visual or auditory (*10*)], the principles of cortical map organization described here may be common to other developing sensory systems.

REFERENCES AND NOTES

1. V. B. Mountcastle, *J. Neurophysiol.* **20**, 408–434 (1957).
2. P. Rakic, *Science* **241**, 170–176 (1988).
3. D. H. Hubel, T. N. Wiesel, *J. Physiol.* **160**, 106–154 (1962).
4. P. Rakic, A. E. Ayoub, J. J. Breunig, M. H. Dominguez, *Trends Neurosci.* **32**, 291–301 (2009).
5. A. Tiriac, B. E. Smith, M. B. Feller, *Neuron* **100**, 1059–1065.e4 (2018).
6. T. K. Hensch, *Annu. Rev. Neurosci.* **27**, 549–579 (2004).
7. P. Gaspar, N. Renier, *Curr. Opin. Neurobiol.* **53**, 43–49 (2018).
8. H. P. Killackey, G. Belford, R. Ryugo, D. K. Ryugo, *Brain Res.* **104**, 309–315 (1976).
9. T. A. Woolsey, J. R. Wann, *J. Comp. Neurol.* **170**, 53–66 (1976).
10. V. Moreno-Juan *et al*., *Nat. Commun.* **8**, 14172 (2017).
11. T. A. Woolsey, H. Van der Loos, *Brain Res.* **17**, 205–242 (1970).
12. A. Agmon, L. T. Yang, E. G. Jones, D. K. O'Dowd, *J. Neurosci.* **15**, 549–561 (1995).
13. J. W. Yang *et al*., *Cereb. Cortex* **23**, 1299–1316 (2013).
14. H. Mizuno *et al*., *Cell Rep.* **22**, 123–135 (2018).
15. O. Mitrukhina, D. Suchkov, R. Khazipov, M. Minlebaev, *Cereb. Cortex* **25**, 3458–3467 (2015).
16. N. Alagem, M. Dvir, E. Reuveny, *J. Physiol.* **534**, 381–393 (2001).
17. J. Wagner, H. J. Luhmann, *Neuropharmacology* **51**, 848–857 (2006).
18. D. P. Calderon, N. Leverkova, A. Peinado, *J. Neurosci.* **25**, 1737–1749 (2005).
19. H. Mizuno *et al*., *Neuron* **82**, 365–379 (2014).
20. R. S. Erzurumlu, P. Gaspar, *Eur. J. Neurosci.* **35**, 1540–1553 (2012).
21. H. Li *et al*., *Neuron* **79**, 970–986 (2013).
22. N. Narboux-Nême *et al*., *J. Neurosci.* **32**, 6183–6196 (2012).
23. H. Van der Loos, T. A. Woolsey, *Science* **179**, 395–398 (1973).
24. W. L. Weller, J. I. Johnson, *Brain Res.* **83**, 504–508 (1975).
25. L. Lokmane, S. Garel, *Semin. Cell Dev. Biol.* **35**, 147–155 (2014).
26. M. C. Crair, R. C. Malenka, *Nature* **375**, 325–328 (1995).

ACKNOWLEDGMENTS

We thank L.M. Rodríguez, R. Susín, and B. Andrés for technical support; T. Iwasato for providing the TCA-GFP mouse; A. Barco for advice on the behavioral experiments; R. Morris, S. Tole, M. Maravall, and D. Jabaudon for critical reading of the manuscript; and the López-Bendito laboratory for stimulating discussions. **Funding:** This work was supported by grants from the European Research Council (ERC-2014-CoG-647012) and the Spanish Ministry of Science, Innovation and Universities (BFU2015-64432-R and Severo Ochoa grant SEV-2017-0723). N.A.-B. held an FPI fellowship from the MINECO. H.G. held postdoctoral fellowships from the Swedish Research Council and the Swedish Brain Foundation. **Author contributions:** N.A.-B., A.S.-F., M.V., and G.L.-B. designed the experiments. N.A.-B., A.S.-F., T.G.-V., F.J.M., and L.P.-S. performed the analysis. N.A.-B. conducted calcium imaging, tracing experiments, and the cFos assays. A.S.-F. conducted calcium imaging and the electrophysiology. T.G.-V. conducted the in vivo calcium imaging. F.J.M. performed the Matlab analysis. L.P.-S. and F.J.M. performed the in vivo multi-electrode recordings. H.G. generated the Kir-mCherry mouse and pioneered Th^{Kir} analysis. A.F. designed, performed, and analyzed initial spontaneous thalamic calcium imaging. G.L.-B. acquired funding. M.V. and G.L.-B. wrote the paper. **Competing interests:** None declared. **Data and materials availability:** All the data in the paper are presented in the main text or supplementary materials.

SUPPLEMENTARY MATERIALS

science.sciencemag.org/content/364/6444/987/suppl/DC1
Materials and Methods
Figs. S1 to S15
References (*27*–*31*)
Movies S1 to S12

12 November 2018; resubmitted 22 March 2019
Accepted 23 April 2019
Published online 2 May 2019
10.1126/science.aav7617

Prenatal activity from thalamic neurons governs the emergence of functional cortical maps in mice

Noelia Antón-Bolaños, Alejandro Sempere-Ferràndez, Teresa Guillamón-Vivancos, Francisco J. Martini, Leticia Pérez-Saiz, Henrik Gezelius, Anton Filipchuk, Miguel Valdeolmillos and Guillermina López-Bendito

Science **364** (6444), 987-990.
DOI: 10.1126/science.aav7617originally published online May 2, 2019

Brain map of touch sensation

The brain's somatosensory cortex contains a topographical map that reflects touch sensation inputs. During embryonic development, axons from the midbrain thalamus build columnar connections to the cortex in the absence of sensory input. Working in mice, Antón-Bolaños *et al.* found that these thalamocortical connections are responsible for organizing the somatosensory cortex (see the Perspective by Tiriac and Feller). Organization of the map in the cortex depends on spontaneous calcium waves in the embryonic thalamus. Thus, the somatosensory map is sketched out before actual sensory input begins to refine the details.

Science, this issue p. 987; see also p. 933